Published in final edited form as:
Nanomedicine (Lond). 2014 February ; 9(2): 253–266. doi:10.2217/nnm.13.22.

Antimicrobial photodynamic therapy with decacationic monoadducts and bisadducts of [70]fullerene: *in vitro* and *in vivo* studies

Liyi Huang[1,2,3], **Min Wang**[4], **Tianhong Dai**[2,3], **Felipe F Sperandio**[2,5], **Ying-Ying Huang**[2,3,6], **Yi Xuan**[2,7], **Long Y Chiang**[4], and **Michael R Hamblin**[*,2,3,8]

[1]Department of Infectious Diseases, First Affiliated College & Hospital, Guangxi Medical University, Nanning, 530021, China

[2]Wellman Center for Photomedicine, Massachusetts General Hospital, Boston, MA 02114, USA

[3]Department of Dermatology, Harvard Medical School, Boston, MA 02115, USA

[4]Department of Chemistry, University of Massachusetts, Lowell, MA 01854, USA

[5]Department of Oral Pathology, School of Dentistry, University of Sao Paulo, Sao Paulo, SP 05508-000, Brazil

[6]Aesthetic & Plastic Center of Guangxi Medical University, Nanning, China

[7]Tufts University, Medford, MA 02155, USA

[8]Harvard-MIT Division of Health Sciences & Technology, Cambridge, MA 02139, USA

Abstract

Background—Antimicrobial photodynamic therapy uses photosensitizers designed to bind to microorganisms and generate reactive oxygen species when illuminated with visible light.

Materials & method—We synthesized a highly water-soluble [70]fullerene monoadduct, $C_{70}[>M(C_3N_6^+C_3)_2]$-$(I^-)_{10}$ (LC17), and bisadduct, $C_{70}[>M(C_3N_6^+C_3)_2][>M(C_3N_6C_3)_2]$ (LC18), both with a well-defined decacationic quaternary ammonium iodide moiety with ten positive charges per C_{70} to give water solubility and bacterial binding. We determined the antimicrobial effects against human pathogens, Gram-positive (*Staphylococcus aureus*) and Gramnegative species (*Escherichia coli* and *Acinetobacter baumannii*) when activated by UVA or white light.

*Author for correspondence: Tel.: +1 617 726 6182, Fax: +1 617 726 8566, hamblin@helix.mgh.harvard.edu.

Ethical conduct of research

The authors state that they have obtained appropriate institutional review board approval or have followed the principles outlined in the Declaration of Helsinki for all human or animal experimental investigations. In addition, for investigations involving human subjects, informed consent has been obtained from the participants involved.

Financial & competing interests disclosure

This work was supported by NIH R01CA137108 and R01AI050875. T Dai was supported by an Airlift Research Foundation Extremity Trauma Research Grant (grant 109421) and a Basic Research Grant from the Orthopaedic Trauma Association (grant 2012-16), and FF Sperandio by CAPES Foundation, Ministry of Education of Brazil (grant number 0310-11-5). The authors have no other relevant affiliations or financial involvement with any organization or entity with a financial interest in or financial conflict with the subject matter or materials discussed in the manuscript apart from those disclosed.

No writing assistance was utilized in the production of this manuscript.

Results—White light was more effective with LC17, while UVA light was more effective with LC18. Both compounds were effective in a mouse model of Gram-negative third-degree burn infections determined by bioluminescence imaging.

Discussion & conclusion—We propose that the attachment of an additional deca(tertiary-ethylenylamino)malonate arm to C_{70} allowed the moiety to act as a potent electron donor and increased the generation yield of hydroxyl radicals under UVA illumination.

Keywords

antimicrobial photodynamic therapy; bioluminescence imaging; decacationic C_{70} fullerene; deca(tertiaryamino)malonate arm; hydroxyl radical; mouse model of burn infection; singlet oxygen

---

Antimicrobial photodynamic therapy (PDT) uses photosensitizers (PS) designed to bind to microorganisms and generate reactive oxygen species (ROS) when illuminated with visible light, which kill the microorganisms by nonspecific oxidative damage [1–3]. This mechanism of action gives the approach a broad spectrum of activity to kill all known classes of microorganisms. The technique has attracted increasing attention due to the relentless and ever-increasing spread of antibiotic resistance not only amongst bacteria (Gram positive, Gram negative and mycobacteria), but also viruses [4], fungi [5] and parasites [6]. In fact, several commentators have referred to the present time as 'the end of the antibiotic era' [7–9]. Antimicrobial PDT can be applied *in vivo*, for instance in animal models of localized infections, provided care is taken to ensure selectivity of binding of the PS between microbial cells and host mammalian cells [10]. One way of increasing binding and penetration of PS to microbial cells and increasing selectivity of killing microbes over host cells is to design PS with a large number of cationic charges [11]. The reasons for this structural requirement are threefold. Firstly, all known classes of microbial cells have pronounced negative charges on their outer surface that provide rapid and strong binding with cationic PS [11]. Secondly, Gram-negative bacteria have a double-membrane cell-wall structure that can be disrupted by polycations allowing better penetration of the PS into the bacterial cell [12]. Thirdly, mammalian cells take up polycationic molecules by the relatively slow process of adsorptive endocytosis, so if light is delivered soon after application of the cationic PS to the infected tissue, the desired selectivity for bacteria in tissue can be achieved [13]. A pronounced increase in the number of charges on the PS molecule may not always increase the efficiency of the PS in antimicrobial PDT [14,15] if these charges serve solely for the purpose of targeting bacteria. However, we have recently demonstrated the use of these multiple cationic charges to carry the same number of iodide atoms as counter anions to improve type I photochemistry by allowing a photoinduced electron-transfer mechanism from the iodide to the fullerene cage [16]. Accordingly, an analogous compound carrying a large number of charges with a large number of associated iodides may be a better PS.

Fullerenes are closed carbon cage molecules whose system of delocalized π-electrons imparts a large absorption of visible light and which have a good quantum yield of a long-lived triplet electronic excited state [17]. They can produce ROS via both the type II photochemical pathway (singlet oxygen) and the type I photochemical pathway (hydroxyl radicals) [18]. Furthermore, they have a high degree of photostability compared with PS based on the tetrapyrrole or phenothiazinium backbones. Moreover, the broad absorption spectrum allows them to be excited with a range of wavelengths ranging from UVA (360 nm) to red (635 nm). For these reasons fullerenes have recently attracted significant amounts of interest [19,20] as PS to mediate PDT of infections as well as cancer. Since fullerenes are highly insoluble in biological media they must be chemically functionalized to provide

water solubility and to prevent aggregation [21]. Attachment of addends containing a large number of cationic charges therefore plays a dual role of bacterial targeting and providing water solubility.

The fullerene C_{70} monoadduct exhibits higher molar optical absorption extinction coefficients than its C_{60} analog at 380–600 nm. The capability of hydrophilic C_{70} monoadducts to absorb more photon energy should increase correspondingly the photoinduced PDT activity during light activation in the same wavelength range. The tertiary amino-based functional group with two unpaired electrons located on the nitrogen atom is electron rich in the presence of the electron-accepting C_{70} cage. Electron transfer from a tertiary amine to C_{70} can be activated by irradiation at short-visible and UVA to UVB wavelengths, leading to the formation of a anionic $(C_{70})^{-}\cdot$ radical and the corresponding cationic amine radical. The former anionic fullerene is then capable of transferring one electron to O_2 resulting in the production of a superoxide radical ($O_2^{-}\cdot$). Accordingly, we proposed the use of a high number (ten) of tertiary amino groups linked and bound on C_{70} as two *N*,*N*′,*N*,*N*,*N*,*N*hexapropyl- hexa(aminoethyl)amido)malonate arms for enhancing $O_2^{-}\cdot$ production, and subsequently to hydroxyl radical (HO·) in biological media, during PDT treatments. The hypothesis is that $^1O_2$ can diffuse more easily into porous cell walls of Gram-positive bacteria to reach sensitive sites, while the less permeable Gram-negative bacterial cell wall needs the more reactive HO· to cause real damage.

The objective of the present study was to compare two C_{70} fullerene derivatives: one with an attached decacationic side chain (LC17) and another with the same decacationic side chain plus an additional deca tertiary amine side chain (LC18) as antimicrobial PS against Grampositive and Gram-negative bacteria. Excitation with both white and UVA light was compared. A mouse model of third-degree burn infection with bioluminescent Gram-negative bacteria was used to test the *in vivo* effectiveness of the therapeutic approach using the more effective UVA excitation.

Materials & methods

Full synthetic methods for di(*tert*-butyl) [70]fullerenyl malonate, $C_{70}[>M(t\text{-}Bu)_2]$; bis (20-oxo-4,7,10,13,16 -pent apropyl - 4,7,10,13,16,19-hexaazatricosan-23-yl)[70] fullerenyl malonate quaternary ammonium iodide salt, $C_{70}[>M(C_3N_6{}^{+}C_3)_2]$-$(I^{-})_{10}$ (LC17); and deca(tertiary-ethylenylamino)malonated decacat ionic bi s(20-oxo-4,7,10,13,16-pentapropyl-4,7,10,13,16,19-hexaaza-tricosan-23-yl)[70]fullerenyl malonate methyl quaternary ammonium iodide salt, $C_{70}[>M(C_3N_6{}^{+}C_3)_2]$ $[>M(C_3N_6C_3)_2]$ (LC18) are provided in the Supplementary material (see online at www.futuremedicine.com/doi/suppl/10.2217/nnm.13.22). Spectroscopic characterization details are also given in the Supplementary material.

Light sources

A broad-band white light source (400–700 nm band pass filter; Lumacare, Newport Beach, CA, USA) was used to deliver light over a spot diameter of 3 cm at an irradiance of 100 mW/cm^2 as measured with a power meter (model DMM 199 with 201 standard head; Coherent, Santa Clara, CA, USA). An ultraviolet A lamp (360 ± 20 nm; American Ultraviolet Co., Lebanon, IN, USA) delivered light in a spot diameter of 15 cm at an irradiance of 30 mW/cm^2 measured using a model IL-1700 research radiometer/photometer (International Light, Inc., Newburyport, MA, USA) over the wavelength range of 250 to 400 nm.

Production of ROS using fluorescent probes

The fluorescent probes used, hydroxyphenyl fluorescein (HPF; H36004) and Singlet Oxygen Sensor Green (SOSG; S36002), were from Molecular Probes, Life Technologies (New York, NY, USA). LC17 and LC18 were dissolved in phosphate-buffered saline (PBS) containing 5-μM probes in wells in a 96-well clear microplate (353072; BD Falcon, San Jose, CA, USA). The total volume of each well added up to 100 μl and the plates were then irradiated with the UVA or white light sources as described above. The fluorescence emission was measured (SpectraMax M5; Molecular Devices, Sunnyvale, CA, USA) using excitation/emission wavelengths of 490/515 nm, as the fluences increased up to 0.5 J/cm^2 for the UVA group and up to 5.0 J/cm^2 for the white light group. Experiments were repeated three times.

Bacterial strains & culture conditions

The bioluminescent bacteria used in this study were as follows: Gram-positive *Staphylococcus aureus* 8325-4 (XEN 8.1) and Gram-negative *E. coli* EPEC WS2572 (XEN 14) and *Acinetobacter baumannii* ATCC BAA 747. *Escherichia coli* EPEC WS2572 (XEN 14) with stable constitutively expressed transposon-mediated integration of lux operon were a kind gift from Xenogen Corp (Alameda, CA, USA). *A. baumannii* ATCC BAA 747 was transduced with a plasmid containing the lux CDABE operon (originally cloned from *Photorhabdus luminescens*) as previously described [22]. The bacteria were routinely grown in brain–heart infusion (BHI) broth (Fisher Scientific, Braintree, MA, USA) with aeration in an orbital shaking incubator at 130 rpm at 37°C overnight to stationary phase. An aliquot of this suspension was then refreshed in fresh BHI to mid-log phase. Cell numbers were estimated by measuring the optical density at 600 nm (optical density of 0.5 = 10^8 colony forming units [CFU]/ml) for all three bacterial species.

Photodynamic inactivation studies

Suspensions of bacteria (10^8 CFU/ml) were incubated in the dark at room temperature for 30 min with various concentrations of LC17 or LC18 (0.1–10 μM for *S. aureus*, 0.1–100 μM for *E. coli* and *A. baumannii*) in pH 7.4 PBS. 1.0-ml aliquots were transferred to a 24-well plate and illuminated from the top of the plates at room temperature with 10 J/cm^2 of UVA or 100 J/cm^2 of white light. Cells treated with LC17 or LC18 in the dark were covered with aluminum foil and incubated for the same time as the PDT groups (30 min). The cells incubated with the lowest concentration of fullerene and then illuminated acted as a light alone control. At the completion of illumination (or dark incubation), aliquots (100 μl) were taken from each well to determine CFU. Care was taken to ensure that the contents of the wells were mixed thoroughly before sampling, as bacteria can settle at the bottom. The aliquots were serially diluted tenfold in PBS to give dilutions of 10^{-1} to 10^{-5} times in addition to the original concentration and 10-μl aliquots of each of the dilutions were streaked horizontally on square BHI agar plates as described by Jett *et al.* [23]. Plates were streaked in triplicate and incubated for 12–18 h at 37°C in the dark to allow colony formation. Each experiment was performed at least three times.

Survival fractions were routinely expressed as ratios of CFUs of microbial cells treated with light and LC17 or LC18 (or LC17 or LC18 in the absence of light) to CFUs of microbes treated with neither.

In vitro PDT studies with mammalian (HeLa) cells

A human cervical cancer cell line, HeLa, was obtained from ATCC (Manassas, VA, USA). The cells were cultured in RPMI-1640 medium with L-glutamine and $NaHCO_3$ (Gibco-Invitrogen, Carlsbad, CA, USA) supplemented with 10% heat-inactivated fetal bovine serum

and penicillin (100 U/ml; Sigma, St Louis, MO, USA) at 37°C in 5% CO_2-humidified atmosphere in 75-cm^2 flasks (Falcon-Invitrogen, Carlsbad, CA, USA). When the cells reached 80% confluence, they were washed with PBS and harvested with 2 ml of 0.25% trypsin-EDTA solution (Sigma). Cells were then centrifuged and counted in trypan blue to ensure viability and plated at a density of 5000/ well in flat-bottom 96-well plates (Fisher Scientific, Pittsburgh, PA, USA). On the following day, dilutions of LC17 and LC18 were prepared in PBS. These dilutions (1–16 μM) were added to the cells and incubated for 30 min. The dimethylacetamide (DMA) concentration in the medium did not exceed 0.2%. The PBS was replaced with complete medium, and 100 J/cm^2 of white light was delivered. The light spot covered four wells, which were considered as one experimental group illuminated at the same time. Control groups were as follows: no treatment, light alone, and dark control with fullerene dilutions described above. Following PDT treatment the cells were returned to the incubator overnight. A 4-h MTT assay [24] was carried out the next day and read at 562 nm using a microplate spectrophotometer (Spectra Max 340 PC; Molecular Devices). Experiments were repeated three times.

Animals

All animal procedures were approved by the Subcommittee on Research Animal Care (IACUC) of Massachusetts General Hospital and met the guidelines of the NIH. Adult female BALB/c mice (Charles River, Wilmington, MA, USA), 6–8 weeks old and weighing 17–21 g, were used in the study. The animals were housed one per cage and maintained on a 12-h light/dark cycle under a room temperature of 21°C with access to food and water *ad libitum*. Mice were divided into groups of n = 6 mice per group and there were five groups for the *E. coli* study, and six groups for *A. baumannii* study, plus mice for the initial optimization studies.

Creation of burn injury & bacterial infection

Before the creation of burns, the mice were anesthetized by intraperitoneal (ip.) injection of a ketamine–xylazine cocktail and shaved on the dorsal surfaces. Burns were created by applying a single preheated (≈95°C) brass block (Small Parts, Inc., Miami, FL, USA) to the dorsal surface of each mouse for 10 s, resulting in a nonlethal, full-thickness, third-degree burn. The brass block area was 10 × 10 mm, giving an area of 100 mm^2 and corresponding to 2.5% of the total body surface area. Immediately after the creation of the burns, the mice were resuscitated with ip. injections of 0.5-ml sterile saline (Phoenix Scientific, Inc., St. Joseph, MO, USA) to prevent dehydration. At 5 min after the creation of burns (allowing the cooling down of the burns), a suspension (50 μl) of bacteria in sterile PBS containing 1.5×10^8 CFU for *E. coli* or 5×10^7 CFU for *A. baumannii* was inoculated onto the surface of each burn with a yellow-tipped pipette and was then smeared onto the burn surface with an inoculating loop. The mice were imaged with the luminescence camera immediately after applying the bacteria to ensure that the bacterial inoculum applied to each burn was consistent.

Bioluminescence imaging

The low-light imaging system (Hamamatsu Photonics KK, Bridgewater, NJ, USA) consists of an intensified CCD camera mounted in a light-tight specimen chamber, fitted with a light-emitting diode, a set-up that allowed for a background gray-scale image of the entire mouse to be captured. By accumulating many images containing binary photon information (an integration time of 2.0 min was used), a pseudo-color luminescence image was generated. Superimposition of this image onto the grayscale background image yielded information on the location and intensity in terms of photon number. The camera was also connected to a computer system through an image processor (Argus-50; Hamamatsu Photonics). Argus-50

control program (Hamamatsu Photonics) was used to acquire images and to process the image data collected.

Prior to imaging, mice were anesthetized by ip. injections of a ketamine–xylazine cocktail. Mice were then placed on an adjustable stage in the specimen chamber, and the wounds were positioned directly under the camera. A gray-scale background image of each wound was made, and this was followed by a photon count of the same region. This entire wound photon count was quantified as relative luminescence units and was displayed in a false color scale ranging from pink (most intense) to blue (least intense).

In vivo PDT

10 min after application of the *E. coli* bacteria to the burns, 100 μl of LC17 or LC18 solution at a concentration of 80 μM in PBS containing 8% v/v DMA was applied to the surface of the burn and smeared over the total burned area. The mice were again imaged using a luminescence camera 30 min after the addition to allow the LC17 or LC18 to bind to and penetrate the bacteria, and any dark toxicity to the bacteria was quantified. Mice were then illuminated with UVA at an irradiance of 30 mW/cm^2 as described above. An aluminum foil template was constructed to expose the burn and a 0.5-cm margin of normal tissue around the burn. Mice were given total fluences of up 72 J/cm^2 for UVA light in aliquots (6, 12, 24, 48 and 72 J/cm^2) with luminescence imaging taking place after each aliquot of light. Immediately after PDT, the mice were resuscitated with a second ip. injection of 0.5-ml sterile saline to prevent dehydration.

In the *A. baumannii* studies, the infected burns were treated as above with 100 μl of LC17 or LC18 solution at a concentration of 300 μM in PBS containing 15% v/v DMA. UVA illumination (72 J/cm^2) was then delivered all at once. There were six groups each of six mice: A: no fullerene, no light, no DMA; B: UVA + DMA; C: LC17 + DMA; D: LC18 + DMA; E: LC17 + DMA + UVA; F: LC18 + DMA + UVA. Aliquots of light with periodic imaging were not used in this case as the initial application of fullerene in DMA resulted in a significant loss of bioluminescence. In this case the mice were imaged daily to quantify the recurrence of the bioluminescence.

Mouse follow-up

The mice were anesthetized by ip. injection of a ketamine–xylazine cocktail and the bacterial luminescence from the mouse burns was recorded daily until the bioluminescence disappeared or the animals were determined to be moribund and euthanized.

Statistics

Values are means of three separate experiments, and bars presented in the graphs are standard errors of the means. Differences between means were tested for significance by one-way analysis of variance and Tukey *post-hoc* test. $p < 0.05$ were considered significant.

Results

Optical absorption spectra of LC17 & LC18

The PDT efficacy can be correlated by the quantum yield of ROS production by [70]fullerene derivatives. High quantum efficiency can be achieved by a combination of two events as: large absorption extinction coefficients at the wavelength range of light applied sufficient to initiate photoexcitation of the C_{70} cage from its ground state to the corresponding singlet excited state; and a high yield of intersystem crossing from this singlet excited state to the triplet excited state. The latter often occurs in a quantitative yield for many fullerene monoadducts. Therefore, absorption extinction coefficient becomes a crucial

parameter for determining suitability of a light source for PDT treatment using a particular PS. Accordingly, we measured UV– visible spectra of $C_{70}[>M(C_3N_6^+C_3)_2]$ (LC17) and $C_{70}[>M(C_3N_6^+C_3)_2][>M(C_3N_6C_3)_2]$ (LC18) in dimethylformamide at the concentration of 2.0×10^{-5} M and correlated their spectral profiles to the emission peak of several UVA and visible light sources used in this study, as shown in Figure 1.

The absorption characteristics of LC17 (Figure 1B) and LC18 (Figure 1C) were found to vary from that of the parent monoadduct $C_{70}[>M(t\text{-Bu})_2]$ (Figure 1A, in $CHCl_3$) with the disappearance of all characteristic C_{70} bands into a featureless curve even though all three compounds share the same monofunctionalized C_{70} cage. The difference implied the occurrence of cage cluster formation of LC17 and LC18 in polar solvent.

Several extinction coefficients (ε) of LC17 and LC18 recorded at λ_{max} of the light applied are summarized in Table 1. The values for LC18 were consistently 2.8–3.0-fold lower than those for LC17 using the white light. In the case of the UVA light, the value is 1.4-fold lower. Based on the area of overlap of the UV–visible spectrum profiles of LC17 and LC18 with the emission band of white and UVA lights, we estimated the relative area integration over the wavelength range at the half-peak width of the light emission band with the value shown in Table 1. The results also revealed a similar trend showing a consistently 2.8-fold lower value for LC18 than those of LC17 using the white light. In the case of the UVA light, the value is 1.5-fold lower. All these optical absorption differences were applied in the correlation of relative PDT efficacy between LC17 and LC18 described below.

ROS production measured by fluorescence probes

ROS generation by fullerenes in PBS solution illuminated by either UVA light (360 ± 20 nm) or white light (400–700 nm) was assessed by fluorescent probes that have been reported to be (reasonably) specific for singlet oxygen (SOSG) or for hydroxyl radical (HPF) [25,26]. The results are shown in Figure 2 where it can be seen that we used ten-times higher fluences of white light than UVA light, as the absorption spectra of the compounds were ten-times higher in the UVA than in the visible spectra regions. Furthermore, the rate of ROS generation is much higher for LC18 than for LC17 (compare Figure 2A with Figure 2B, and Figure 2C with Figure 2D). As the absorption spectrum is comparable for both these molecules, the difference in ROS generation is likely to be due to differences in the aggregation state in aqueous solution. Because LC18 has the second set of arms attached, it is likely to aggregate less than LC17 because of added steric hindrance preventing fullerene molecules coming together. For singlet oxygen production white light gives a higher rate than UVA light for both LC17 and LC18. However, although white light provides a greater rate of hydroxyl radical production than UVA light for LC17, the opposite is the case for LC18, where UVA light gives a higher rate than white light. These differences were significant ($p < 0.05$).

PDT killing of *S. aureus*, *A. baumannii* & *E. coli* by LC17 or LC18 excited by white light or UVA light

Figure 3 shows the survival fraction curves obtained against the Gram-positive bacterium *S. aureus* or Gram-negative bacteria *A. baumannii* and *E. coli* incubated for 30 min with various concentration of LC17 or LC18. The bacterial suspensions were illuminated with 10 J/cm^2 of UVA light or with 100 J/cm^2 of white light, due to differences in the absorption spectra as described above. All species were eradicated (greater than 6.0 logs or 99.9999% killing) with the appropriate concentrations of fullerene. For the Gram-positive *S. aureus*, LC17 (Figure 3A) showed significantly more killing when excited with white light compared to UVA light, but for LC18 (Figure 3B) the killing was identical. For the Gram-negative *A. baumannii*, identical killing was obtained for both light wavelengths for both

LC17 (Figure 3C) and LC18 (Figure 3D). Interestingly, for another Gram-negative species, *E. coli*, although both wavelengths gave the same killing when LC17 was employed (Figure 3E), when LC18 (Figure 3F) was used, there was significantly more killing with UVA light than was found with white light. There was only small toxicity (<1 log) with light alone, as can be seen by inspecting the survival fraction of the PDT groups at the lowest fullerene concentration tested (0.1 μM for *S. aureus* and 1 μM for the Gram-negative bacteria). LC17 exhibited more dark toxicity against Gram-negative species than LC18, giving 2–4 logs of killing at 100 μM, but there were still 3–4 logs more killing under illumination.

Selectivity for bacteria over mammalian cells

In order to demonstrate selective killing of bacterial cells compared with mammalian cells we incubated the human carcinoma cell line (HeLa) with fullerenes under the same conditions (30 min incubation in PBS) as were employed for bacterial cells and illuminated the cells with either 10 J/cm^2 of UVA light or 100 J/ cm^2 of white light. Figure 4 shows that for both LC17 (Figure 4A) and LC18 (Figure 4B) there was only a small amount of PDT killing (up to 30%) as determined by the MTT assay. It should be noted that if the incubation was much longer (6–24 h) then significantly more killing of mammalian cells might be expected.

In vivo PDT treatment of mouse third-degree burns infected with *E. coli*

We tested the *in vivo* PDT activity of these fullerenes in a mouse model of a third-degree burn infected with Gram-negative bioluminescent bacterial species. We initially used the pathogenic variant of *E. coli* (EPEC) and inoculated the burns with 1.5×10^8 CFUs. We used UVA light, as judged by the results in Figure 3, and overall this wavelength appeared to be the most effective in killing all the tested species. After considerable experimentation we settled on an 80-μM solution of fullerene in PBS containing 8% v/v DMA. The DMA solvent is important in keeping the fullerene in solution and encouraging penetration of the PS into the infected tissue of the burn. The light dose-dependent reduction of bioluminescent signal is shown in Figure 5. It can be seen in Figure 5A that UVA plus PBS containing 8% DMA (no fullerene) as a light alone control gave only a slight reduction in bioluminescent signal even after 72 J/ cm^2 of light had been delivered. When LC17 was used (Figure 5B) there was a significant reduction in bioluminescence signal apparent at 48 J/cm^2 and only a trace remaining after 72 J/cm^2. When LC18 was used (Figure 5C) it can be seen there was a noticeable drop in signal after only 12 J/cm^2 had been delivered, and by the time 72 J/cm^2 had been delivered the signal had been effectively eliminated. There was no significant reduction in bioluminescence after application of either LC17 or LC18 without light exposure as a dark control (data not shown). The average bioluminescence signals as quantified by Argus software for the three groups (n = 6 mice per group) are shown in Figure 6. The values from both PDT groups were significantly lower than values from the UVA control at all fluences, and the bioluminescence values from mice treated with LC18 were significantly lower than the corresponding values from LC17 at 12, 24 and 48 J/cm^2.

When these mice were examined on succeeding days (days 1–6) it was apparent that the bacterial infection had recurred in the burns, and despite the successful PDT on day 0, there was no significant difference in bioluminescence signal between treatment and control groups on days 1–6 (data not shown).

In vivo PDT treatment of mouse third-degree burn infected with *A. baumanii*

Because we observed recurrence of the *E. coli* in the mouse burn in the days following the PDT treatment, we asked whether a therapeutically useful single PDT treatment could be demonstrated. We formed the hypothesis that the recurrence observed with PDT of *E. coli* was due to a combination of factors. Firstly, that a few remaining viable bacteria were left in

the burn even after disappearance of the luminescence signal. Secondly, that the virulence of the bacteria was an important factor. To overcome these adverse factors we changed several parameters in the experiment. Firstly, we changed to *A. baumannii*, which although is clinically problematic due to its high antibiotic resistance, appears to be less virulent in this mouse model and we used a lower inoculum (5×10^7 compared with 1.5×10^8). Secondly, we raised the concentration of fullerene from 80 to 300 μM. Thirdly, we raised the concentration of DMA from 8 to 15%. Figure 7 shows the bioluminescence signals of representative mice captured daily from days 0 (before PDT) to day 6 post-PDT. It can be seen that the absolute control (Figure 7A, no light, no fullerene, no DMA) showed a continuing infection in the burn that lasted for 6 days. All other groups (Figures 7B–7F) showed a loss of bioluminescence signal on day 1 (the day after PDT). However, in the three control groups (UVA alone [Figure 7B], LC17 dark control [Figure 7C], and LC18 dark control [Figure 7D]) there was significant recurrence of bioluminescence on day 2 that lasted until day 6. In the LC17 PDT group (Figure 7E) there was only a tiny amount of recurrence visible at day 4 that remained minute on days 5 and 6. In the LC18 PDT group there was no recurrence of bioluminescence visible on any day of follow-up.

Discussion & conclusion

We have shown that decacationically armed C_{70} fullerenes are highly effective broad-spectrum selective antibacterial PS that are able to kill 6 logs of both Gram-positive and Gram-negative bacteria *in vitro*. Furthermore, these compounds can have therapeutic effects in mouse models of hard-to-treat Gram-negative bacterial burn infections.

It is known that fullerenes are able to generate ROS via both type I (hydroxyl radicals) and type II (singlet oxygen) photochemical mechanisms [18,27]. We formed the hypothesis that by attaching a second arm containing ten tertiary amine groups that could act as electron donors, we could increase the proportion of hydroxyl radical generation, which is thought to occur initially by electron transfer from the excited fullerene to molecular oxygen to form a superoxide radical anion [28,29]. The fluorescent probe experiments provided some evidence to support this hypothesis. The large increase in activity of LC18 versus LC17 was attributed to reduced aggregation due to the steric hindrance provided by the second arm preventing fullerene molecules coming together. In fact, we can envision that the likely hydrophobic– hydrophobic interactions between the second deca(tertiary-ethylenylamino)malonate arm and C_{70} cage in PBS solution should force the deca-amino arm to wrap around the cage moiety resembling a molecular encapsulation of C_{70}. In this event, we would expect an intrinsic molecular photophysical behavior of fullerenes without the interference of self-quenching effect and bimolecular triplet–triplet annihilation processes of $^3(C_{70}>)^*$ in the aggregated form of either [70]fullerene monoadducts or bisadducts [30]. Disregarding the deca-amino arm, we proposed that the mechanism led to the generation of hydroxyl radicals by LC17 and LC18 under visible irradiation raised from a sequential reaction of $^1O_2$ with iodide anion (I^-) consistent with the reported phenomena [31]. When HPF detection of hydroxyl radicals was compared it can be seen that LC18 had more activation with UVA light versus white light, while the reverse was the case with LC17. It appears that electron transfer reactions are favored when the more energetic UVA photons are used to excite the fullerene molecule.

LC17 was able to kill more Gram-positive *S. aureus* when it was excited by white light than when it was excited by UVA light, which are conditions that are hypothesized to favor generation of singlet oxygen. We have recently obtained evidence [32] that Gram-positive bacteria are relatively more susceptible to singlet oxygen than Gram-negative bacteria. There are reports in the literature that also support this hypothesis [33–36]. The explanation may be that the porous cell wall structure of Gram-positive bacteria allows singlet oxygen to

penetrate more easily than the less permeable cell wall of Gram-negative bacteria. The Gram-negative *A. baumannii* was killed equally by fullerenes excited by UVA light and by white light, although LC17 did appear to be somewhat more effective than LC18 (which was the opposite to the finding for *E. coli).* Although *A. baumannii* is Gram negative, it has been shown by several reports [37–40] to be sensitive to PDT treatments, possibly because its permeability barrier is less permeable than other Gram negatives such as *E. coli*, and singlet oxygen can therefore more readily diffuse inside. Further study with a wider range of Gram-negative species is needed to confirm this hypothesis. LC18 killed a higher number of *E. coli* when excited by UVA light, which are conditions that are hypothesized to favor generation of hydroxyl radicals. Martin and Logsdon [41] reported that *E. coli* was particularly susceptible to killing by photosensitizing dyes that generated hydroxyl radicals upon illumination. Although it is broadly accepted that singlet oxygen is the most important ROS that mediates microbial cell death in antimicrobial PDT [42], recent emerging evidence suggests that type I radical mechanisms have been relatively overlooked. Not only fullerenes [32], but phenothiazinium dyes [43] have also been shown to involve type I photochemistry and hydroxyl radicals. It is entirely feasible that UVA-1 light could be used in clinical applications; for example, Mang and Krutmann [44] have reported that fluences as high as 130 J/cm^2 have been used to treat atopic dermatitis and psoriasis in patients.

Our laboratory has reported that several different functionalized fullerenes can act as broad-spectrum antimicrobial PS. The most important structural feature for high activity appears to be the number of quaternary amino groups. A study by Tegos *et al.* [45] showed that a tricationic C_{60} fullerene was more effective than a mono- or di-cationic derivative in the photoinactivation of Gram-positive and Gramnegative bacteria, and fungi. Huang *et al.* [46] found that a hexacationic derivative was most effective. Mizuno *et al.* [47] reported that a tetracationic C_{60} derivative was highly effective in photoinactivating microbial cells.

In order for antimicrobial PDT treatments to advance into the clinic it is necessary to show that the PS are able to mediate selective killing of bacteria while preserving the viability of host mammalian cells. We were able to show that when HeLa cells were treated under the same conditions that killed several logs of bacterial cells, only a comparatively small loss of viability (30%) was observed. It should be noted that HeLa is a cancer cell line that may not be the most suitable for this purpose, and that primary human fibroblasts may need to be studied in further experiments. The fact that a short incubation time was employed is critical, as these large polycationic molecules, such as LC17 and LC18, are taken up into mammalian cells by the slow process of endocytosis. Therefore, if a short drug–light interval is used for treatment of an infection, damage to the surrounding normal tissue should be minimized.

Third-degree burns are particularly susceptible to bacterial infection as the barrier function of the skin is destroyed, the dead tissue is devoid of host-defense elements, and a systemic immune suppression is a worrying consequence of serious burns [48]. Furthermore, the lack of perfusion of the burned tissue means that systemic antibiotics are generally ineffective [49]. Although excision and skin grafting is now standard treatment for third-degree burns [50], superimposed infection is still a major problem. Patients with Gram-negative burn infections have a higher likelihood of developing sepsis than Grampositive infections [51]. Topical antimicrobials are the mainstay of therapy for burn infections and PDT may have a major role to play in the management of this disease [52].

We obtained good light dose-dependent loss of bioluminescence signal in the mouse model of *E. coli* burn infection, and LC18 was more effective than LC17 in mediating PDT under UVA illumination, consistent with the *in vitro* results. Further studies using white light as well as UVA light in this mouse model of PDT of burn infection would be desirable.

However, despite this success, recurrence of bioluminescence was observed in the succeeding days. While it is entirely possible that the PDT treatment could be repeated each day until the infection was defeated, we considered that it would be preferable if a single PDT treatment could be shown to be effective in eliminating the bacteria from the burn. This goal was achieved with an *A. baumannii* model, which is of high clinical relevance as this species has been found to be the most prevalent in a military burns hospital [53] and is notorious for its antibiotic resistance [54]. Again, LC18 was found to be superior to LC17 in this application of PDT for burn infection. How can we explain the lack of bioluminescence signal at day 1 in groups B, C, and D as well as in groups E and F? We believe that this is an effect of the DMA solvent used to deliver the fullerene and also used together with the UVA light. However, the DMA does not necessarily completely kill the bacteria but temporarily reduces the bioluminescence signal, which explains why no signal is seen at day 1 in UVA + DMA (B) and in both dark controls (C and D). The fact that regrowth is found in these groups of mice (B, C and D) while those treated with actual PDT did not exhibit regrowth (E and F) does suggest that either the bacteria were not really killed in groups B, C and D, and could therefore regrow, or alternatively that the bacteria were completely killed in groups E and F and thus could not be imaged using bioluminescence, and could not regrow because they were all dead.

Lu *et al.* [55] reported an *in vivo* study where a tricationic C_{60} fullerene excited by white light was used to treat a mouse model of excisional wound infection by Gram-negative *Pseudomonas aeruginosa* or *Proteus mirabilis.* This is a highly invasive infection model and fullerene-mediated PDT was able to save the lives of mice infected with *P. mirabilis* and, in the case of *P. aeruginosa*, when used in combination with subtherapeutic doses of antibiotics (tobramycin).

Supplementary Material

Refer to Web version on PubMed Central for supplementary material.

References

Papers of special note have been highlighted as:

▪ of interest

▪ ▪ of considerable interest

1. Hamblin, MR.; Jori, G. Photodynamic Inactivation of Microbial Pathogens: Medical and Environmental Applications. RSC Publishing; Cambridge, UK: 2011.

2▪ ▪. Hamblin MR, Hasan T. Photodynamic therapy: a new antimicrobial approach to infectious disease? Photochem Photobiol Sci. 2004; 3(5):436–450. Highly cited review of photodynamic therapy (PDT) for infections. [PubMed: 15122361]

3. Hamblin, MR.; Mroz, P. Advances in Photodynamic Therapy: Basic, Translational and Clinical. Artech House; Norwood, MA, USA: 2008.

4. Costa L, Faustino MA, Neves MG, Cunha A, Almeida A. Photodynamic inactivation of mammalian viruses and bacteriophages. Viruses. 2012; 4(7):1034–1074. [PubMed: 22852040]

5. Calzavara-Pinton P, Rossi MT, Sala R, Venturini M. Photodynamic antifungal chemotherapy. Photochem Photobiol. 2012; 88(3):512–522. [PubMed: 22313493]

6. Baptista MS, Wainwright M. Photodynamic antimicrobial chemotherapy (PACT) for the treatment of malaria, leishmaniasis and trypanosomiasis. Braz J Med Biol Res. 2011; 44(1):1–10. [PubMed: 21152709]

7. Nordmann P, Poirel L, Toleman MA, Walsh TR. Does broad-spectrum β-lactam resistance due to NDM-1 herald the end of the antibiotic era for treatment of infections caused by Gram negative bacteria? J Antimicrob Chemother. 2011; 66(4):689–692. [PubMed: 21393184]
8. Yoshikawa TT. Antimicrobial resistance and aging: beginning of the end of the antibiotic era? J Am Geriatr Soc. 2002; 50(Suppl 7):S226–S229. [PubMed: 12121517]
9. Bell SG. Antibiotic resistance: is the end of an era near? Neonatal Netw. 2003; 22(6):47–54. [PubMed: 14700181]
10. Huang L, Dai T, Hamblin MR. Antimicrobial photodynamic inactivation and photodynamic therapy for infections. Methods Mol Biol. 2010; 635:155–173. [PubMed: 20552347]
11. Sharma SK, Dai T, Kharkwal GB, et al. Drug discovery of antimicrobial photosensitizers using animal models. Curr Pharm Des. 2011; 17:1303–1319. [PubMed: 21504410]
12. Merchat M, Spikes JD, Bertoloni G, Jori G. Studies on the mechanism of bacteria photosensitization by meso-substituted cationic porphyrins. J Photochem Photobiol B. 1996; 35(3):149–157. [PubMed: 8933721]
13. Huang L, Huang YY, Mroz P, et al. Stable synthetic cationic bacteriochlorins as selective antimicrobial photosensitizers. Antimicrob Agents Chemother. 2010; 54(9):3834–3841. [PubMed: 20625146]
14. Alves E, Costa L, Carvalho CM, et al. Charge effect on the photoinactivation of Gramnegative and Gram-positive bacteria by cationic meso-substituted porphyrins. BMC Microbiol. 2009; 9:70. [PubMed: 19368706]
15. Pereira JB, Carvalho EF, Faustino MA, et al. Phthalocyanine thio-pyridinium derivatives as antibacterial photosensitizers. Photochem Photobiol. 2012; 88(3):537–547. [PubMed: 22332603]
16▪. Wang M, Huang L, Sharma SK, et al. Synthesis and photodynamic effect of new highly photostable decacationically armed [60]- and [70]fullerene decaiodide monoadducts to target pathogenic bacteria and cancer cells. J Med Chem. 2012; 55(9):4274–4285. Describes the synthesis and *in vitro* application of decacationic fullerenes to photodestroy bacteria and cancer cells. [PubMed: 22512669]
17. Arbogast JW, Darmanyan AP, Foote CS, et al. Photophysical properties of C_{60}. J Phys Chem A Mol Spectrosc Kinet Environ Gen Theory. 1991; 95(1):11–12.
18▪. Yamakoshi Y, Umezawa N, Ryu A, et al. Active oxygen species generated from photoexcited fullerene (C_{60}) as potential medicines: O_2^{-}* versus $^1O_2$. J Am Chem Soc. 2003; 125(42):12803–12809. One of the first papers showing that photoactivated fullerenes produce type I photochemistry as typified by superoxide as well as type II photochemistry typified by singlet oxygen. [PubMed: 14558828]
19. Mroz P, Tegos GP, Gali H, Wharton T, Sarna T, Hamblin MR. Photodynamic therapy with fullerenes. Photochem Photobiol Sci. 2007; 6(11):1139–1149. [PubMed: 17973044]
20▪ ▪. Sharma SK, Chiang LY, Hamblin MR. Photodynamic therapy with fullerenes *in vivo*: reality or a dream? Nanomedicine (Lond). 2011; 6(10):1813–1825. Covers all the instances where fullerenes have been used to mediate PDT of cancer and of infections *in vivo*. [PubMed: 22122587]
21. Nakamura E, Isobe H. Functionalized fullerenes in water. The first 10 years of their chemistry, biology, and nanoscience. Acc Chem Res. 2003; 36(11):807–815. [PubMed: 14622027]
22. Dai T, Lu Z, Huang L, et al. Photodynamic therapy for *Acinetobacter baumannii* burn infections in mice. Antimicrob Agents Chemother. 2009; 53:3929–3934. [PubMed: 19564369]
23. Jett BD, Hatter KL, Huycke MM, Gilmore MS. Simplified agar plate method for quantifying viable bacteria. Biotechniques. 1997; 23(4):648–650. [PubMed: 9343684]
24. Merlin JL, Azzi S, Lignon D, Ramacci C, Zeghari N, Guillemin F. MTT assays allow quick and reliable measurement of the response of human tumour cells to photodynamic therapy. Eur J Cancer. 1992; 28A(8–9):1452–1458. [PubMed: 1387543]
25▪. Price M, Reiners JJ, Santiago AM, Kessel D. Monitoring singlet oxygen and hydroxyl radical formation with fluorescent probes during photodynamic therapy. Photochem Photobiol. 2009; 85(5):1177–1181. Introduces the use of specific fluorescent probes to distinguish between type I and type II photochemical mechanisms in PDT. [PubMed: 19508643]

26. Setsukinai K, Urano Y, Kakinuma K, Majima HJ, Nagano T. Development of novel fluorescence probes that can reliably detect reactive oxygen species and distinguish specific species. J Biol Chem. 2003; 278(5):3170–3175. [PubMed: 12419811]
27. Zhao B, He YY, Bilski PJ, Chignell CF. Pristine (C_{60}) and hydroxylated [$C_{60}(OH)_{24}$] fullerene phototoxicity towards HaCaT keratinocytes: type I vs type II mechanisms. Chem Res Toxicol. 2008; 21(5):1056–1063. [PubMed: 18422350]
28. Ashur I, Goldschmidt R, Pinkas I, et al. Photocatalytic generation of oxygen radicals by the water-soluble bacteriochlorophyll derivative WST11, noncovalently bound to serum albumin. J Phys Chem A. 2009; 113(28):8027–8037. [PubMed: 19545111]
29. Dabrowski JM, Arnaut LG, Pereira MM, et al. Combined effects of singlet oxygen and hydroxyl radical in photodynamic therapy with photostable bacteriochlorins: evidence from intracellular fluorescence and increased photodynamic efficacy *in vitro*. Free Radic Biol Med. 2012; 52(7): 1188–1200. [PubMed: 22285766]
30. Riggs JE, Sun YP. Optical limiting properties of [60]fullerene and methano[60]fullerene derivative in solution versus in polymer matrix: the role of bimolecular processes and a consistent nonlinear absorption mechanism. J Phys Chem A. 1999; 103:485–495.
31. Gupta AK, Rohatgi-Mukherjee KK. Solvent effect on photosensitized oxidation of iodide ion by anthracene sulphonates. Photochem Photobiol. 1978; 27:539–543.
32. Huang L, Xuan Y, Koide Y, Zhiyentayev T, Tanaka M, Hamblin MR. Type I and type II mechanisms of antimicrobial photodynamic therapy: an *in vitro* study on Gram-negative and Gram-positive bacteria. Lasers Surg Med. 2012; 44(6):490–499. [PubMed: 22760848]
33. Dahl TA, Midden WR, Hartman PE. Comparison of killing of Gram-negative and Gram-positive bacteria by pure singlet oxygen. J Bacteriol. 1989; 171(4):2188–2194. [PubMed: 2703469]
34. Sabbahi S, Alouini Z, Jemli M, Boudabbous A. The role of reactive oxygen species in *Staphylococcus aureus* photoinactivation by methylene blue. Water Sci Technol. 2008; 58(5): 1047–1054. [PubMed: 18824803]
35. Vakrat-Haglili Y, Weiner L, Brumfeld V, et al. The microenvironment effect on the generation of reactive oxygen species by Pdbacteriopheophorbide. J Am Chem Soc. 2005; 127(17):6487–6497. [PubMed: 15853357]
36. Valduga G, Bertoloni G, Reddi E, Jori G. Effect of extracellularly generated singlet oxygen on Gram-positive and Gram-negative bacteria. J Photochem Photobiol B. 1993; 21(1):81–86. [PubMed: 8289115]
37. Ragas X, Dai T, Tegos GP, Agut M, Nonell S, Hamblin MR. Photodynamic inactivation of *Acinetobacter baumannii* using phenothiazinium dyes: *in-vitro* and *in-vivo* studies. Lasers Surg Med. 2010; 42(5):384–390. [PubMed: 20583252]
38. Dai T, Tegos GP, Lu Z, et al. Photodynamic therapy for *Acinetobacter baumannii* burn infections in mice. Antimicrob Agents Chemother. 2009; 53(9):3929–3934. [PubMed: 19564369]
39. Nitzan Y, Ashkenazi H. Photoinactivation of *Acinetobacter baumannii* and *Escherichia coli* B by a cationic hydrophilic porphyrin at various light wavelengths. Curr Microbiol. 2001; 42(6):408–414. [PubMed: 11381332]
40. Nitzan Y, Balzam-Sudakevitz A, Ashkenazi H. Eradication of *Acinetobacter baumannii* by photosensitized agents *in vitro*. J Photochem Photobiol B. 1998; 42(3):211–218. [PubMed: 9595710]
41▪. Martin JP, Logsdon N. The role of oxygen radicals in dye-mediated photodynamic effects in *Escherichia coli* B. J Biol Chem. 1987; 262(15):7213–7219. Demonstrates that hydroxyl radicals are important in PDT killing of Gram-negative bacteria. [PubMed: 3034885]
42. Maisch T, Baier J, Franz B, et al. The role of singlet oxygen and oxygen concentration in photodynamic inactivation of bacteria. Proc Natl Acad Sci USA. 2007; 104(17):7223–7228. [PubMed: 17431036]
43▪ ▪. Huang L, St Denis TG, Xuan Y, et al. Paradoxical potentiation of methylene bluemediated antimicrobial photodynamic inactivation by sodium azide: role of ambient oxygen and azide radicals. Free Radic Biol Med. 2012; 53(11):2062–2071. First demonstration of the potentiation of antimicrobial PDT by the addition of azide rather than the expected inhibition by singlet oxygen quenching. [PubMed: 23044264]

44. Mang R, Krutmann J. UVA-1 phototherapy. Photodermatol Photoimmunol Photomed. 2005; 21(2): 103–108. [PubMed: 15752130]
45. Tegos GP, Demidova TN, Arcila-Lopez D, et al. Cationic fullerenes are effective and selective antimicrobial photosensitizers. Chem Biol. 2005; 12(10):1127–1135. [PubMed: 16242655]
46. Huang L, Terakawa M, Zhiyentayev T, et al. Innovative cationic fullerenes as broadspectrum light-activated antimicrobials. Nanomedicine. 2010; 6(3):442–452. [PubMed: 19914400]
47. Mizuno K, Zhiyentayev T, Huang L, et al. Antimicrobial photodynamic therapy with functionalized fullerenes: quantitative structure–activity relationships. J Nanomedic Nanotechnol. 2011; 2(2):109–117.
48. Sharma BR. Infection in patients with severe burns: causes and prevention thereof. Infect Dis Clin North Am. 2007; 21(3):745–759. ix. [PubMed: 17826621]
49. Ollstein RN, Mcdonald C. Topical and systemic antimicrobial agents in burns. Ann Plast Surg. 1980; 5(5):386–392. [PubMed: 6779699]
50. Saffle JR. Closure of the excised burn wound: temporary skin substitutes. Clin Plast Surg. 2009; 36(4):627–641. [PubMed: 19793557]
51. Kang CI, Kim SH, Park WB, et al. Bloodstream infections caused by antibiotic-resistant Gramnegative bacilli: risk factors for mortality and impact of inappropriate initial antimicrobial therapy on outcome. Antimicrob Agents Chemother. 2005; 49(2):760–766. [PubMed: 15673761]
52. Dai T, Huang YY, Sharma SK, Hashmi JT, Kurup DB, Hamblin MR. Topical antimicrobials for burn wound infections. Recent Pat Antiinfect Drug Discov. 2010; 5(2):124–151. [PubMed: 20429870]
53. Keen EF 3rd, Robinson BJ, Hospenthal DR, et al. Incidence and bacteriology of burn infections at a military burn center. Burns. 2010; 36(4):461–468. [PubMed: 20045259]
54. Asadollahi P, Akbari M, Soroush S, et al. Antimicrobial resistance patterns and their encoding genes among *Acinetobacter baumannii* strains isolated from burned patients. Burns. 2012; 38(8): 1198–1203. [PubMed: 22579564]
55▪ ▪. Lu Z, Dai T, Huang L, et al. Photodynamic therapy with a cationic functionalized fullerene rescues mice from fatal wound infections. Nanomedicine (UK). 2010; 5(10):1525–1533. First demonstration that antimicrobial PDT mediated by a fullerene can save the life of mice with wound infections.

Future perspective

The present report suggests that antimicrobial PDT may be a promising medical application of fullerenes. The fact that these compounds are applied topically to an infected wound or burn removes many of the concerns attached to systemic administration of fullerenes including nanotoxicology and long retention times in tissues. The finding that an additional deca tertiary amine may act as an electron donor and improve type I photochemistry suggests a new approach in PS design and synthesis. The fact that different wavelengths of excitation can produce different photochemical effects is interesting and deserves more study.

Executive summary

Synthesis & compound design

- We designed and synthesized a highly water-soluble [70]fullerene monoadduct, $C_{70}[>M(C_3N_6{}^+C_3)_2]$-$(I^-)_{10}$ (LC17), and bisadduct, $C_{70}[>M(C_3N_6{}^+C_3)_2][>M(C_3N_6C_3)_2]$ (LC18), each consisting of a well-defined decacationic quaternary ammonium iodide salt of di(*N*,*N*′,*N*,*N*,*N*,*N*-hexapropyl-hexa(aminoethyl)amido)malonate arm.
- Both derivatives possessed ten positive charges per C_{70}, which were proposed to increase water solubility and their ability to target pathogenic Gram-positive and Gram-negative bacterial cells, and enable them to act as broad-spectrum selective antibacterial nanophotodynamic therapy drugs.
- Incorporation of a total of either 12 (for LC17) or 24 (for LC18) attached propyl groups was designed to provide a well-balanced hydrophobicity–hydrophilicity character and to allow possible wrapping around the C_{70} cage moiety to minimize the direct cage–cage contact and self-quenching effect.

Results

- Experimental results showed that white light was more effective with LC17 while UVA light was more effective with LC18.
- Both compounds were effective in a mouse model of Gram-negative third-degree burn infections determined by bioluminescence imaging. Effective *in vivo* activity was demonstrated in a virulent model of *Escherichia coli* burn infection, and a clinically relevant model of *Acinetobacter baumannii* burn infection.

Discussion & conclusion

- The data suggest that the attachment of an additional deca(tertiary-ethylenylamino)malonate arm to C_{70}, producing LC18, allowed the moiety to act as a potent electron donor and increased the generation yield of hydroxyl radicals under UVA illumination. This is consistent with the reported phenomena of photoinduced intramolecular electron transfer from the tertiary amine moiety to the fullerene cage in polar solvents, including water, at the short excitation wavelength.
- With the availability of ten tertiary amine moieties, each capable of donating one electron to the C_{70} cage, LC18 may function as an electron-rich precursor for hydroxyl radical production that demonstrated a new approach in enhancing HO· radical killing of pathogenic bacteria in contrast to the more common $^1O_2$-killing mechanism.

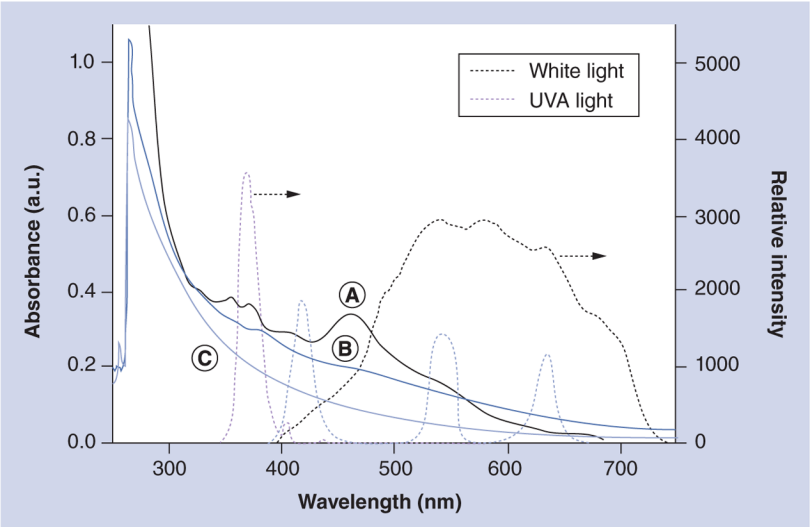

Figure 1. Correlation of UV–visible spectra of fullerenes to the emission spectra of light

(A) $C_{70}[>M(t\text{-}Bu)_2]$; **(B)** $C_{70}[>M(C_3N_6{}^+C_3)_2]\text{-}(I^-)_{10}$ (LC17); and **(C)** $C_{70}[>M(C_3N_6{}^+C_3)_2][>M(C_3N_6C_3)_2]$ (LC18). Samples of **(A)** and **(B)**/**(C)** were prepared in $CHCl_3$ and dimethylformamide, respectively, at a concentration of 2.0×10^{-5} M.

a.u.: Arbitrary unit.

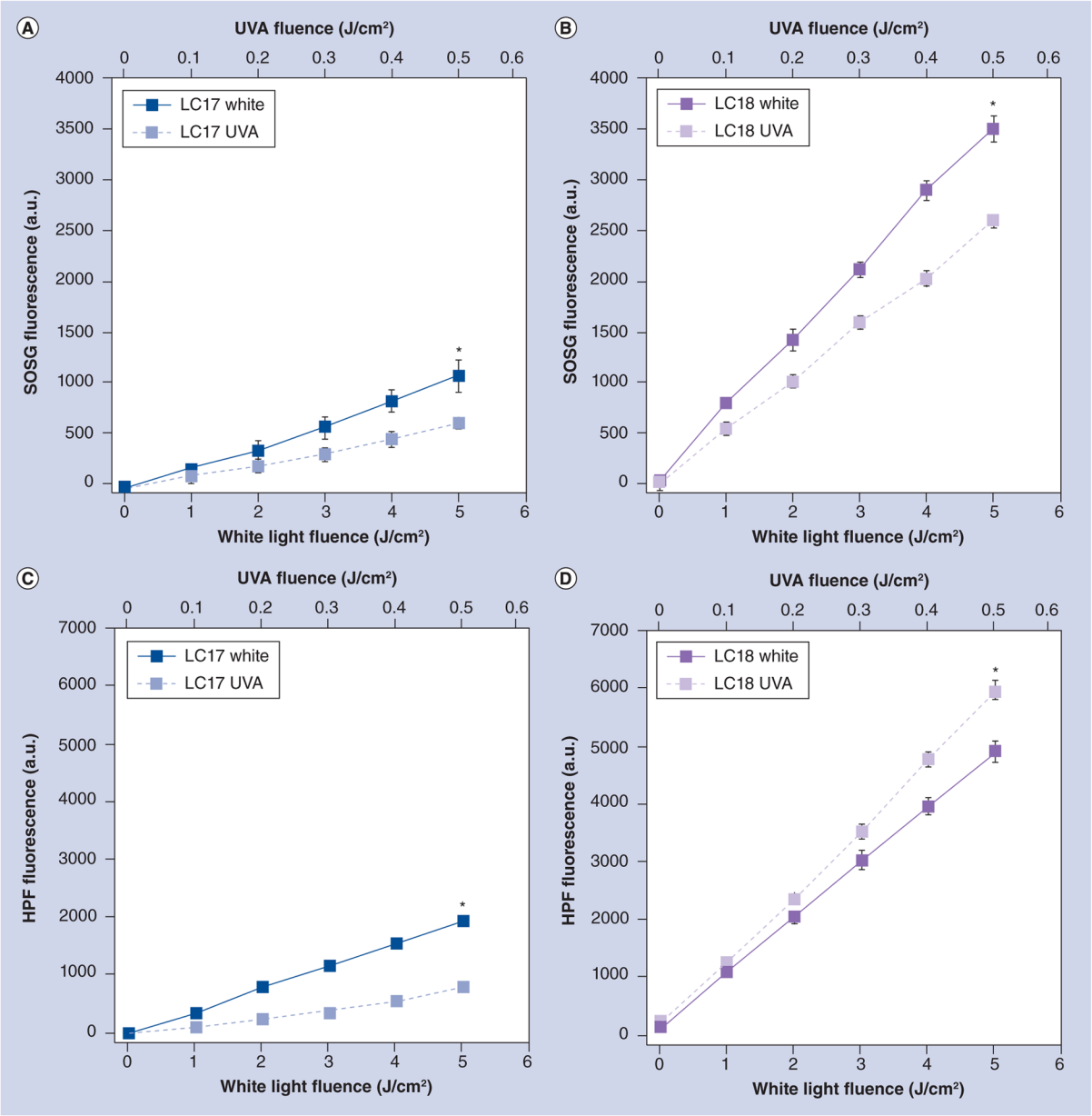

Figure 2. Fluorescent probe activation by fullerenes in phosphate-buffered saline solution illuminated with UVA light or white light

(A) LC17 and SOSG; **(B)** LC18 and SOSG; **(C)** LC17 and HPF; and **(D)** LC18 and HPF.

*$p < 0.05$.

a.u.: Arbitrary unit; HPF: Hydroxyphenyl fluorescein; SOSG: Singlet Oxygen Sensor Green.

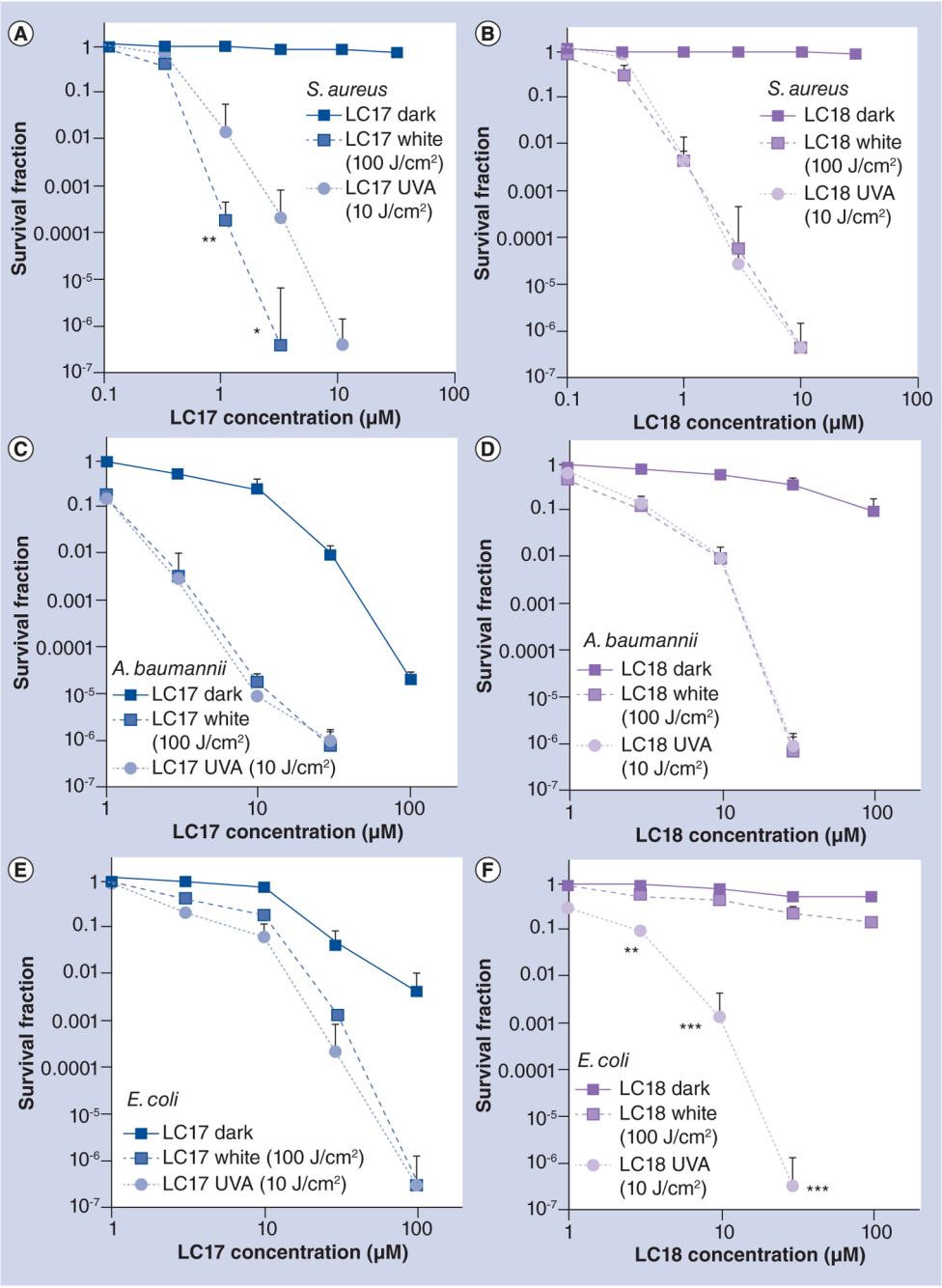

Figure 3. Antimicrobial photoinactivation curves of bacteria incubated with increasing concentrations of fullerenes followed by illumination with white or UVA light

Gram-positive *Staphylococcus aureus* incubated with LC17 **(A)** or LC18 **(B)** and illuminated with UVA light (10 J/cm^2) or white light (100 J/cm^2). Gram-negative *Acinetobacter baumannii* incubated with LC17 **(C)** or LC18 **(D)** and illuminated with UVA light (10 J/cm^2) or white light (100 J/cm^2). Gram-negative *Escherichia coli* incubated with LC17 **(E)** or LC18 **(F)** and illuminated with UVA light (10 J/cm^2) or white light (100 J/cm^2).

*p < 0.05; **p < 0.01; ***p < 0.001.

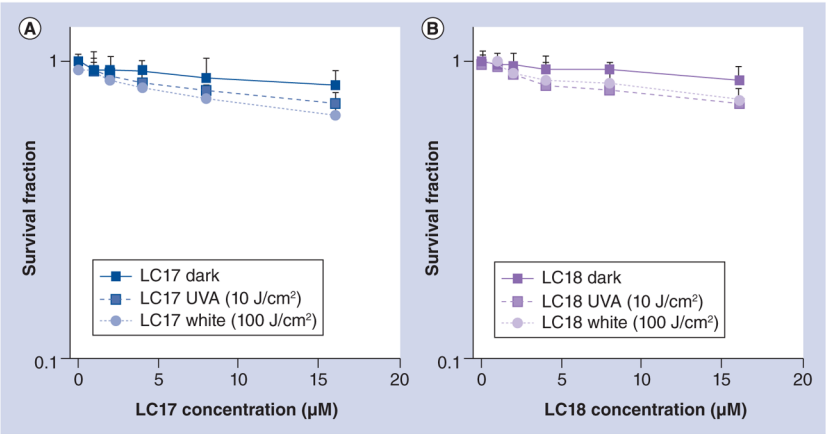

Figure 4. Killing of HeLa mammalian cells by fullerenes incubated under the same condition as bacteria (30 min incubation in phosphate-buffered saline) and illuminated with either UVA light (10 J/cm^2) or white light (100 J/cm^2)

(A) LC17; and **(B)** LC18.

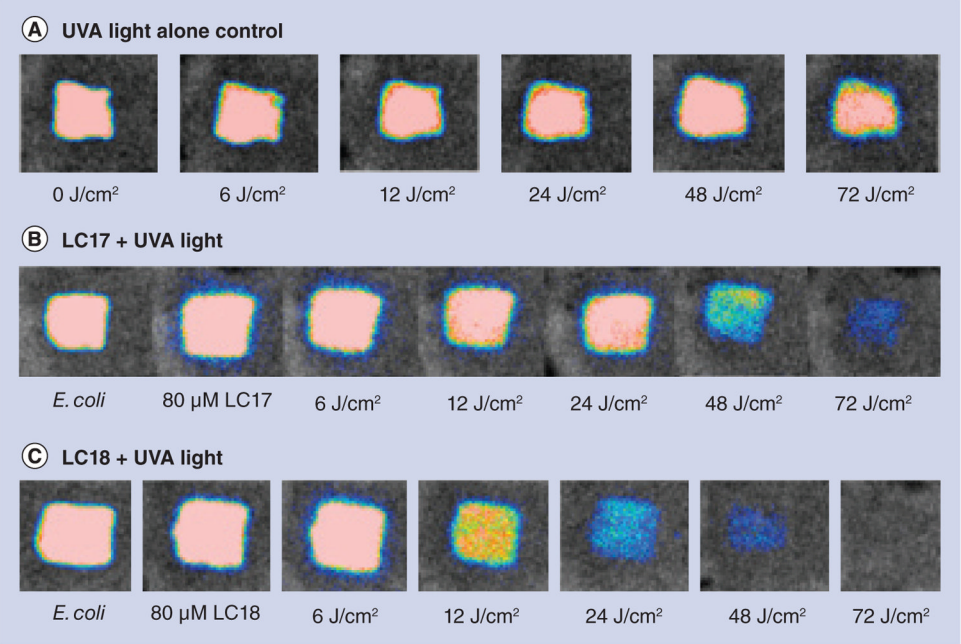

Figure 5. Representative bioluminescence images from mice with *Escherichia coli* burn infections (day 0) and treated with successive fluences of photodynamic therapy or UVA light alone
(A) UVA control; **(B)** LC17 + UVA light; and **(C)** LC18 + UVA light. There was no significant reduction in bioluminescence after application of either LC17 or LC18 without light exposure as a dark control (data not shown).

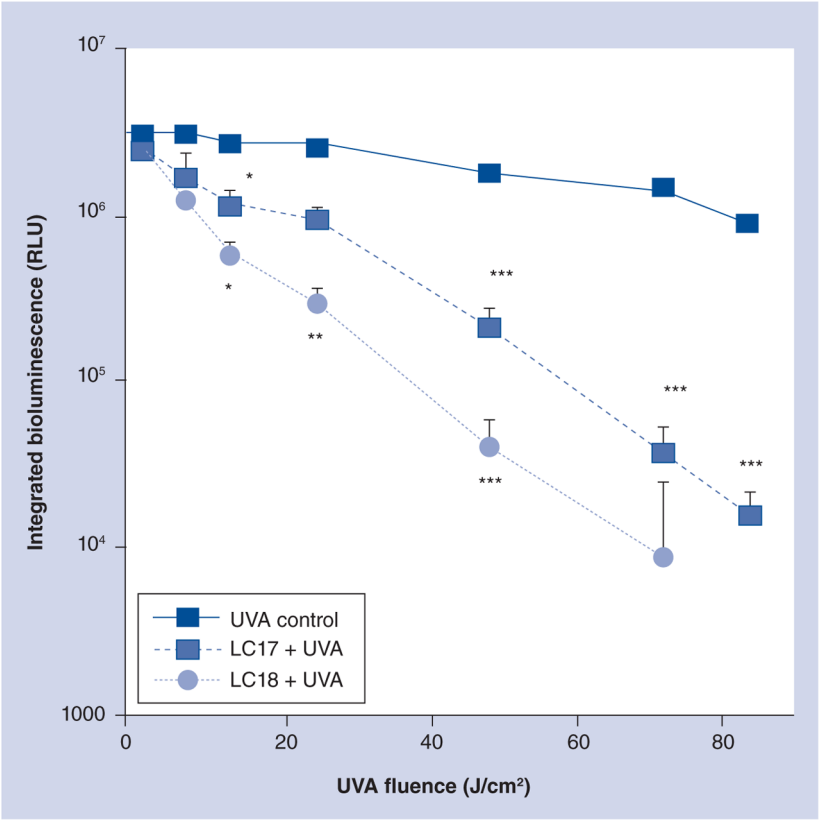

Figure 6. Light dose–response curves of the normalized bioluminescence signals for UVA controls and mice treated with photodynamic therapy

*p < 0.05; **p < 0.01; ***p < 0.001.

RLU: Relative light units.

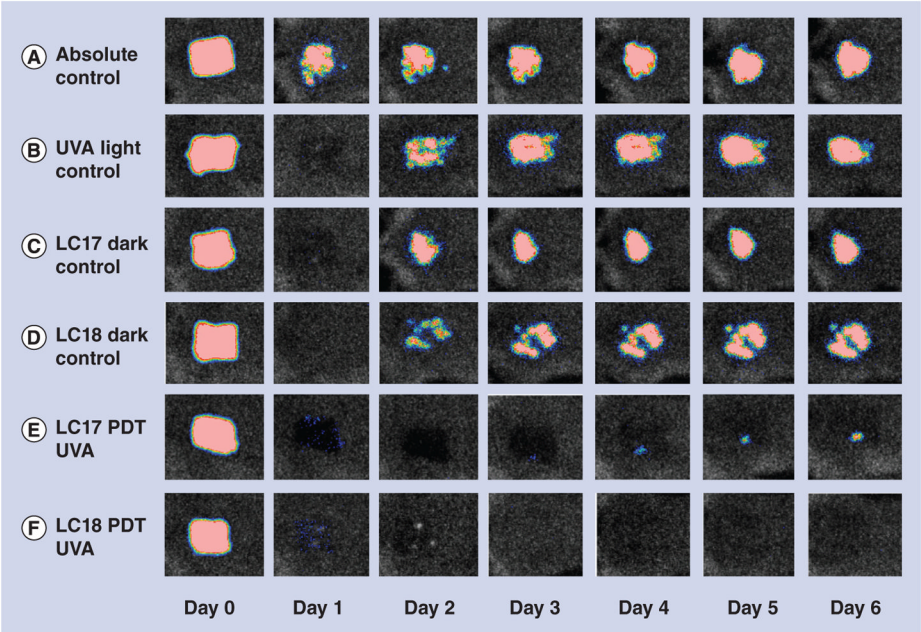

Figure 7. Representative bioluminescence images from mice with *Acinetobacter baumannii* burn infections and treated with photodynamic therapy, UVA light alone or absolute control, captured day 0 (before photodynamic therapy) and then daily for 6 days

(A) Absolute control; **(B)** UVA control + 15% DMA; **(C)** LC17 + 15% DMA; **(D)** LC18 + 15% DMA; **(E)** LC17 + 15% DMA + UVA light; and **(F)** LC18 + 15% DMA + UVA light. DMA: Dimethylacetamide; PDT: Photodynamic therapy.

Table 1

Extinction coefficients† and the relative area integration‡ under UV–visible spectrum profiles of LC17 and LC18.

Compound	ε at 536 nm (white light)	ε at 575 nm (white light)	ε at 368 nm (UVA light)	I_{area} at 479–690 nm (white light)	I_{area} at 361–380 nm (UVA light)
LC17	6.94×10^6	5.50×10^6	1.51×10^7	50.4	12.8
LC18	2.47×10^6	1.83×10^6	1.06×10^7	18.2	8.76

† ε at λ_{max} of the light applied (cm^2/mol).

‡ I_{area} over the wavelength range at the half-peak width of the light emission band.